Ultrafast Mapping of Coherent Dynamics and Density Matrix Reconstruction in a Terahertz-Assisted Laser Field

Yizhu Zhang,[1,2] Tian-Min Yan,[1,*] and Y. H. Jiang[1,3,4,†]

[1]*Shanghai Advanced Research Institute, Chinese Academy of Sciences, Shanghai 201210, China*
[2]*Center for Terahertz waves and College of Precision Instrument and Optoelectronics Engineering,*
Key Laboratory of Opto-electronics Information and Technical Science, Ministry of Education, Tianjin University, China
[3]*University of Chinese Academy of Sciences, Beijing 100049, China*
[4]*ShanghaiTech University, Shanghai 201210, China*

A time-resolved spectroscopic protocol exploiting terahertz-assisted photoionization is proposed to reconstruct transient density matrix. Population and coherence elements are effectively mapped onto spectrally separated peaks in photoionization spectra. The beatings of coherence dynamics can be temporally resolved beyond the pulse duration, and the relative phase between involved states is directly readable from the oscillatory spectral distribution. As demonstrated by a photoexcited multilevel open quantum system, the method shows potential applications for subfemtosecond time-resolved measurements of coherent dynamics with free electron lasers and tabletop laser fields.

Quantum coherence derived from the principle of superposition is a fundamental concept in quantum mechanics and a ubiquitous phenomenon with the time scale ranging from milliseconds, as in delicately prepared cold atoms, to attoseconds for electronic coherence in field-perturbed atoms [1] and molecules [2]. In atoms and molecules, the photoionization induced electronic coherence prepared by shaking the inner-shell electrons has been uncovered to lose within ~ 1 fs. The decoherence is closely related to the correlation between the photoelectron and the parent ion, significantly affecting the formation of coherent hole wave packets [1,2]. As another example, the coherence-assisted energy transfer in photosynthetic complexes, as is explored by the multidimensional optical spectroscopy [3–5], has sparked extensive interest in the role of quantum coherence played in the macroscopic world. The involvement of multiple transport pathways in the extremely complicated biomolecular environment necessitates further supporting evidences from experimental observations of quantum dynamics.

The complete dynamic information of an open quantum system is encoded in the time-evolved density matrix elements $\rho_{ij}(\tau)$, including the population ρ_{ii} and the coherence ρ_{ij} $(i \neq j)$. The $\rho_{ij}(\tau)$-reconstruction from dedicated designed experiments, e.g., the quantum process tomography with the multidimensional spectroscopy [6], is always desirable. The temporal resolution of optical spectroscopy, however, is restricted to tens of femtoseconds. Since quantum states are typically probed by femtosecond-duration pulses, the convolution with the probing pulse leads to the smear of signatures of faster electronic coherences.

In this sense, observing the ultrafast electronic coherence, in principle, requires the attosecond metrology. Exploiting the attosecond transient absorption spectroscopy, the electronic coherence of the valence electron in krypton ions was measured with the subfemtosecond temporal accuracy [7]. The same spectroscopic methodology also allows observing the correlated two-electron coherence motion in helium with attosecond temporal resolution [8]. Although the attosecond metrology can probe the electron wave-packet motion with high temporal resolution, it requires tremendous efforts with sophisticated laser techniques, including the precise control of both the amplitude and phase of the femtosecond light field throughout the measurement. Moreover, contributions from population and coherence are overlapped after one-dimensional spectral projections, thus usually concealing quantum coherence. For the recently developed free-electron-laser (FEL) facilities, the compression of the pulse with high energetic photons [from extreme ultraviolet (XUV) to hard x-ray region] down to the subfemtosecond scale is difficult. Thus, recording the subfemtosecond electronic coherence using a femtosecond probe pulse accompanied by a phase-locked near infrared pulse has been proposed [9]. The sidebands created around the characteristic peaks carry the high-resolution information of coherence, yet simultaneously complicate the spectroscopic analysis due to the possibly contaminated characteristic spectral features. Moreover, the prerequisite that the photon energy of the streaking field has to be resonant with the relevant states may become a restriction.

In this work, we propose a spectroscopic method to retrieve the full information of the density matrix, like the

two-dimensional spectroscopy, unraveling the contributions of coherence in an extra dimension. Exploiting the femtosecond XUV pulse and terahertz (THz) streaking field, we show that density matrix elements directly map into the photoelectron spectra. Especially, the method in principle allows observing the motion of the electronic wave packet in FEL facilities. In contrast to the proposal operating in the so-called "sideband regime" [9], our method works in the "streaking regime" [10]. Moreover, without the restriction that the photon energy must match the energy gap between coherently excited states [9], the method can be applied in systems without *a priori* knowledge. Conventionally, the streaking technique is used to characterize the temporal profile of ultrashort pulses [10–13]. Here, the THz-streaking technique is used to investigate ultrafast dynamics.

For a multilevel open quantum system, the scheme of the streaking-assisted photoionization is illustrated in Fig. 1(a).
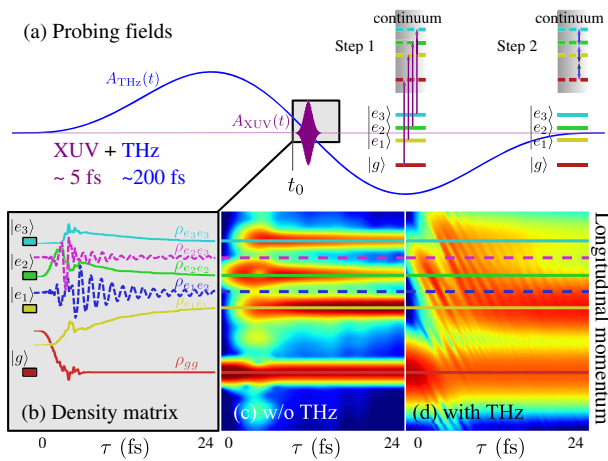

FIG. 1. Schematic of the THz streaking-assisted photoionization experiment that allows for the real-time density matrix imaging. (a) The probing pulse configuration in the measurement. To observe the unknown quantum dynamics of an open quantum system within the temporal window (gray box), a femtosecond XUV pulse (purple) with a well-synchronized THz streaking pulse (blue) as a probe beam scans over time delay τ. The XUV pulse is locked at the zero crossing of the THz vector potential. (b) The energy levels and the time evolution of the density matrix elements ρ_{ij} within the time window. (c) Photoelectron momentum distribution without THz field. Populations ρ_{ii} are mapped into spectral peaks of different longitudinal momentum p, as indicated by colors of solid lines. The τ-dependent spectral yields, labeled by red, yellow, green, and cyan lines for ρ_{gg}, $\rho_{e_1e_1}$, $\rho_{e_2e_2}$, and $\rho_{e_3e_3}$, respectively, reveal the evolution of populations. (d) Photoelectron momentum distribution with THz streaking. Spectral peaks are broadened and the emergent oscillating fringes, labeled along blue and purple dashed lines, can be shown to account for coherences $\rho_{e_1e_2}$ and $\rho_{e_2e_3}$, respectively. The fringe can be well resolved, though the duration of the probing XUV pulse is much longer than its period of oscillation. The effective separation of ρ_{ij} along p and the temporally resolved coherence dynamics allow one to reconstruct the time evolution of ρ_{ij}.

The system is prepared in an initial state at time t_0 with some additional excitation not shown explicitly in the figure. The probe fields, as proposed in this work, comprise a femtosecond XUV pulse and a well-synchronized THz pulse, the zero crossing of whose vector potential is required to be locked at the center of the XUV pulse. As illustrated by the inset of Fig. 1(a), the combination of the two pulses realizes a two-step process. First, the single-photon ionization induced by the XUV pulse liberates the electron of the superposed state at τ, the time delay relative to t_0, taking a frozen snapshot of quantum states exactly at that time. The THz wave then drives the photoelectron, kinetically rearranging electronic trajectories and inducing the interference between trajectories from different states in the final momentum distribution $w(p; \tau)$, which is a critical step to the observation of the coherence. We show that the dynamics of the system at any time τ as described by $\rho_{ij}(\tau)$ [Fig. 1(b)] are mapped directly onto $w(p; \tau)$, with different elements differentiated by longitudinal momentum p. Scanning over τ, the measured $w(p; \tau)$, as shown in Figs. 1(c) and (d), allows for reconstructing the time-evolved $\rho_{ij}(\tau)$. Without the THz field [Fig. 1(c)], spectral peaks depict the time-evolved populations, which can also be measured using other time-resolved techniques. With the THz field [Fig. 1(d)], interference fringes are formed upon broadened peaks, which is of essential concern due to the encoded information of coherence. All details of these figures can be referred to Fig. 3. The further analysis shows that $w(p; \tau)$ is composed of a series of Gaussian peaks corresponding to all $\rho_{ij}(\tau)$, laying the foundation for $\rho_{ij}(\tau)$-reconstruction. The method provides an alternative tool to investigate the decoherence of attosecond photoionization in atoms and molecules, and the coherence energy transport in complex photoreaction systems.

The $w(p; \tau)$ to measure in the experiment can be analyzed under the strong field approximation. Assuming the atom is subject to linearly polarized fields, $E(t) = E_{\text{XUV}}(t) + E_{\text{THz}}(t)$, the ionization signal $w(p; \tau) = |p||M_p(\tau)|^2$ is collected along the polarization direction. Neglecting the high-order above threshold ionization, the amplitude of the direct ionization in the length gauge reads $M_p(\tau) = \lim_{t\to\infty} \int_0^t dt' e^{iS_p(t')} \langle p + A(t')|\hat{\mu}E(t')|\Psi_0(t')\rangle$, where $A(t) = A_{\text{XUV}}(t) + A_{\text{THz}}(t)$ is the vector potential and $S_p(t') = \frac{1}{2}\int_0^{t'} dt''[p + A(t'')]^2$. Note, τ is hidden as the temporal center of pulses in $A(t)$ and $E(t)$. $\hat{\mu}$ is the transition dipole, and $|\Psi_0(t)\rangle$ is the initial (superposition) state. The photoelectron emission process consists of two steps. The laser field first liberates the electron from the atom when the XUV pulse plays a dominant role. Subsequently, the photoelectron is drifted to the final momentum. Since the amplitudes $|A_{\text{XUV}}| \ll |A_{\text{THz}}|$, the free electron is driven dominantly by the THz electric field. According to the analysis of the ionization probability in the streaking regime (see Supplemental Material [14], Sec. I), when amplitudes of

the wave functions vary slowly within the temporal window of the XUV pulse of the peak field amplitude $E_0^{(\text{XUV})}$, the distribution $|M_p(\tau)|^2$ comprises Gaussian peaks for all population and coherence terms, $|M_p(\tau)|^2 = (\pi(E_0^{(XUV)})^2/2|b(p)|)[W_{\text{pop}}(p;\tau) + W_{\text{coh}}(p;\tau)]$, with

$$W_{\text{pop}}(p;\tau) = \sum_i \rho_{ii}(\tau) e^{-(\Omega_{ii}^2(p)/|b(p)\sigma|^2)}, \tag{1}$$

$$W_{\text{coh}}(p;\tau) = 2\sum_{i,j<i} \text{Re}[\rho_{ij}(\tau) e^{i(\alpha p \Omega_{ij}(p)\Delta_{ij}/|b(p)|^2)}]$$
$$\times e^{-(\Omega_{ij}^2(p)/|b(p)\sigma|^2)} e^{-((\Delta_{ij}/2)^2/|b(p)\sigma|^2)}, \tag{2}$$

from which the positions and widths of spectral peaks are easily read. Here, $\Omega_{ij}(p) = p^2/2 + (I_p^{(i)} + I_p^{(j)})/2 - \omega_{\text{XUV}}$, where ω_{XUV} is the photon energy of XUV field and $I_p^{(i)} = -E_i$ is the ionization potential of the ith state. Spectral peaks appear at p where $\Omega_{ij}(p) = 0$, whose solutions include $p_{ii} = \pm\sqrt{2(\omega_{\text{XUV}} - I_p^{(i)})}$ for ρ_{ii}, and $p_{ij} = \pm\sqrt{2(\omega_{\text{XUV}} - (I_p^{(i)} + I_p^{(j)})/2)}$ that is exactly between p_{ii} and p_{jj} for ρ_{ij} $(i \neq j)$. Thus, $\rho_{ij}(\tau)$ in principle can be inferred from $w(p_{ij};\tau)$ at characteristic momentum p_{ij}. The widths of peaks for both W_{pop} and W_{coh} are determined by $|b(p)\sigma| = \sqrt{1/\sigma^2 + (\alpha p\sigma)^2}$ with $b(p) = 1/\sigma^2 - i\alpha p$ dependent on the THz field amplitude α and the temporal width of XUV field σ (standard deviation). In Eq. (2), though W_{coh} is much smaller than W_{pop} due to the presence of the last exponential term of $\Delta_{ij} = I_p^{(i)} - I_p^{(j)}$, the relative amplitude of W_{coh} enhances when the THz field increases. For the energetic spaces spanning over a few eV in typical molecular transitions, the THz electric field of $\sim$ kV/cm, which is conveniently provided by tabletop THz sources nowadays, is sufficient to couple the coherently excited states and reveal W_{coh}.

In the neighborhood of p_{ij}, the exponent in the real part of Eq. (2), $p\Omega_{ij}(p)/|b(p)|^2 \simeq p_{ij}^2(p - p_{ij})/(1/\sigma^4 + \alpha^2 p_{ij}^2)$, is linearly proportional to p. Defining $\varphi_{ij}(\tau) = \Delta_{ij}\tau + \varphi_i - \varphi_j$ the instantaneous relative phase between states i and j, whose initial phases are φ_i and φ_j, respectively, the real part in Eq. (2) becomes $|\rho_{ij}(\tau)|\cos[-\Delta_{ij}\alpha p_{ij}^2(p - p_{ij})/(1/\sigma^4 + \alpha^2 p_{ij}^2) + \varphi_{ij}(\tau)]$, indicating that the spectral yield oscillates with both τ and p. As expected, the oscillatory frequency Δ_{ij} along τ axis agrees with the evolution of $\rho_{ij}(\tau)$ $(i \neq j)$, which can be resolved beyond the duration of the XUV pulse. The oscillation along p axis, however, is noteworthy, since it provides a potential single-τ approach to reconstruct phase $\varphi_{ij}(\tau)$ without the necessity of scanning over time delay τ.

Taking the simplest example of a two-level system, we show the feasibility of coherence imaging and relative-phase reconstruction using the THz-streaking method.

Assuming the system is prepared in the superposition state with the equal probabilities, $|\Psi_0(t)\rangle = (|g\rangle e^{-iE_g(t-t_0)+i\varphi_g} + |e\rangle e^{-iE_e(t-t_0)+i\varphi_e})/\sqrt{2}$, with $|g\rangle$ and $|e\rangle$ the ground state and excited state of energies E_g and E_e, respectively. Here we consider a system with $E_g = -13.6$ eV and $E_e = -3.4$ eV, and initial phases are $\varphi_e = \varphi_g = 0$ at the initial time $t_0 = 0$ fs. The photon energy of the XUV pulse is 2 a.u. (54.4 eV) with the peak field amplitude 0.005 a.u. (intensity $\sim 9 \times 10^{11}$ W/cm^2), and the duration is 5 fs. The center frequency of the single-cycle THz pulse is 4 THz and the peak field strength is 0.001 a.u. ($\sim$5 MV/cm). In principle, the requirement that XUV pulse is temporally locked at the zero crossing of $A_{\text{THz}}(t)$ can be satisfied in the FEL facility, where the XUV and THz pulses, generated by the same electron bunch from the linear accelerator, are well synchronized [12]. The jitter between the excitation pulse and probing FEL pulse is hardly controlled within attosecond accuracy nowadays, but the restriction can be overcome by the continuously developed technique of synchronization. Since there is no need for the single-shot measurement, the reliable statistics of spectra can be provided with state-of-art synchronization of the pulse sequence. In our approach, the Fourier transform limited XUV pulse is required. Although Fourier transformation limited pulse is not conveniently delivered in the self-amplified spontaneous emission (SASE) mode, the seeding operation improves the temporal coherence and the profile of FEL pulse [15].

Scanning the probing fields over τ yields $w(p;\tau)$ as shown in Fig. 2. Panels (a) and (b) show the spectrograms before and after applying the streaking THz field, respectively. As the kinetic energy of the photoelectron from the ith state is $\omega_{\text{XUV}} - I_p^{(i)}$, the spectral peaks at $p_{gg} = 1.73$ a.u. and $p_{ee} = 1.94$ a.u. originate from states $|g\rangle$ and $|e\rangle$, respectively. The two τ-independent peaks recover W_{pop} in Eq. (1) since the amplitudes of $|g\rangle$ and $|e\rangle$ are constants. With the THz field, the two peaks in panel (b) are significantly broadened, and in the intermediate region around $p_{eg} = 1.84$ a.u. fringes are formed. Extracting $w(p = p_{eg};\tau)$, as indicated by the white dashed line in Fig. 2(b), the fringes shown in Fig. 2(c) oscillate with the period 0.4 fs, corresponding to 10.2 eV between states $|g\rangle$ and $|e\rangle$, in good agreement to the oscillatory pattern of coherence $\text{Re}[\rho_{eg}(\tau)]$. Remarkably, the THz-streaking assisted method allows for resolving the subfemtosecond quantum beating that cannot be achieved by a 5-fs probing XUV pulse alone. On the other hand, as depicted by Eq. (2), Fig. 2(d) for $w(p;\tau = t_0)$ also shows the oscillatory behavior with p near $p = p_{eg}$, in good agreement with the sum over analytically derived Gaussian peaks. The p-dependent oscillation allows for the easy reconstruction of relative phase at arbitrary time τ. Comparing with $\varphi_{eg}(t_0) = 0$ in (d), the distribution for $\varphi_{eg}(t_0) = \pi/2$
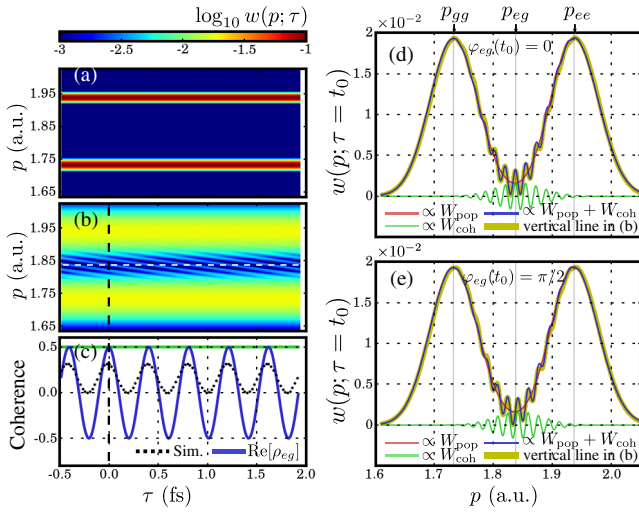
FIG. 2. The temporally resolved quantum coherence with streaking-assisted photoionization. In a two-level system, we assume the amplitudes of the two states are constant with initial relative phase $\varphi_{eg}(t_0) = \varphi_e - \varphi_g = 0$ at $t_0 = 0$ fs. Panels (a) and (b) show $w(p;\tau)$ without and with THz-streaking, respectively. Panel (c) shows both the coherence $\text{Re}[\rho_{eg}(\tau)]$ (blue) and the temporal profile of the simulated spectral signal $w(p = p_{eg};\tau)$ (black dotted line), as extracted along the white dashed line in (b). Panel (d) presents $w(p;\tau = t_0)$ as extracted along the black dashed line in (b). The extracted result (yellow) and the sum over model-based Gaussian peaks (blue), including the contributions from W_{pop} in Eq. (1) (red) and W_{coh} in Eq. (2) (green), are compared. The relative phase $\varphi_{eg}(t_0)$ can be reconstructed with a single-τ measurement at time $\tau = t_0$ simply by examining $w(p;t_0)$ along the p axis. When $\varphi_{eg}(t_0) = 0$, the coherence (green) at $p = p_{eg}$ is maximized as $\cos[\varphi_{eg}(t_0)] = 1$. By comparison, assuming $\varphi_{eg}(t_0) = \pi/2$, the distribution is shown in (e), where the coherence at $p = p_{eg}$ becomes 0.
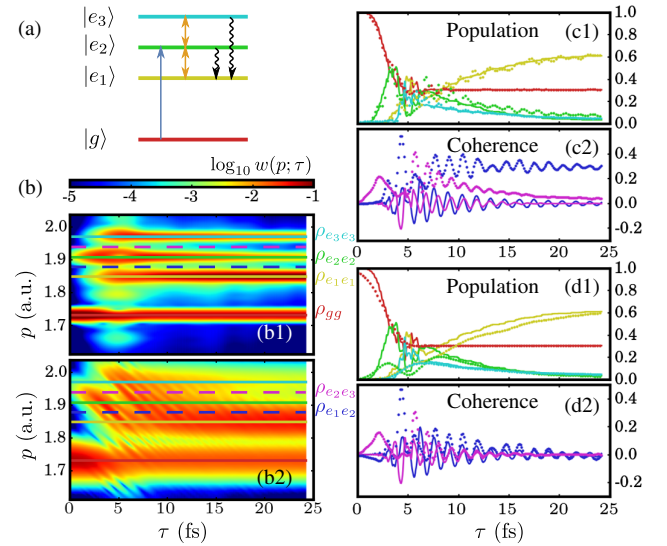
FIG. 3. Reconstruction of $\rho_{ij}(\tau)$ in a multilevel open system. The four-level system under the excitation of two-color fields is shown in (a) with energies $(E_g, E_{e_1}, E_{e_2}, E_{e_3}) = (-0.5, -0.29, -0.18, -0.06)$ a.u.. The initial coherences at time t_0 are generated by, e.g., a two-color pulse sequence, depicted by the gray and orange arrows. Relaxation processes are assumed to occur within the excited manifold, where populations in $|e_2\rangle$ and $|e_3\rangle$ may jump randomly to the lowest excited state $|e_1\rangle$ with constant rates, as shown by the wiggly arrows. Panels (b1) and (b2) show momentum distributions without and with streaking-THz field, respectively. The peaks of characteristic momenta p_{ij}, along which the results are extracted for ρ_{ij}-reconstruction, are indicated by dashed lines of the same color code as used for energy levels in (a). In (c), the THz-streaking signals extracted from (b2) (dotted lines with the same color code) are compared with the true ρ_{ij} (solid lines). Panel (d) shows the $\rho_{ij}(\tau)$ reconstructed with the protocol described in the main text.

presented in (e) indicates that $\varphi_{eg}(t_0)$ can be directly mapped by the phase of oscillatory $w(p;\tau = t_0)$ at $p = p_{eg}$. Note, the fringes near p_{eg} in (b) are not merely caused by the superposition of the broadened peak of W_{pop} at p_{ee} and p_{gg}. According to Eq. (2), there indeed exists the in-between peak at p_{eg} for coherence $W_{\text{coh}}(p_{eg})$ even without THz field, but its relative intensity can be significantly enhanced by the streaking-THz field.

The simple two-level system, as shown in Fig. 2, has demonstrated that $\rho_{ij}(\tau)$ are well embedded in the streaking-assisted $w(p;\tau)$. However, the method is particularly useful when complicated energy structure is involved and the ultrafast relaxation and decoherence dynamics in open quantum systems are of concern. Here, we propose a reconstruction protocol to extract $\rho_{ij}(\tau)$ in an ensemble consisting of four-level atoms that interact with near-resonant pulses [Fig. 3(a)]. Briefly, the protocol consists in measuring two ionization spectra. First, with only XUV field, one is able to extract populations ρ_{ii}. Then, applying the THz field, the acquired coherence-encoded spectrum can be further processed by the known ρ_{ii} to find out the

coherence ρ_{ij}. Further details are provided in Supplemental Material [14], Sec. III. Since the photoionization is evaluated based on the wave function $|\Psi_0(t')\rangle$, the open quantum system is simulated using the method of Monte Carlo wave function (quantum jump; see Supplemental Material [14], Sec. IV) [16], which is equivalent to the Lindblad-type master equation, allowing for the description of spontaneous emission and decoherence.

The THz-free and THz-streaking measurements are shown in Figs. 3(b1) and 3(b2), respectively. Because of the densely spaced energy levels, the relatively weak THz field at 0.0006 a.u. (2 MV/cm) is sufficient to signify $w(p_{e_1 e_2};\tau)$ and $w(p_{e_2 e_3};\tau)$ for coherences between adjacent excited states. All other parameters of the probing fields are the same as used for the two-level system. Note that in Fig. 3(b2) with spectral peaks dramatically broadened by the THz field, beating patterns along τ are all over the spectrogram, including $w(p_{ii};\tau)$ ($i = g, e_1, e_2, e_3$) within the excited manifold. Extracting the simulated result for populations along dashed lines in Fig. 3(b2) at $p = p_{ii}$, these artificial oscillations are clearly seen in Fig. 3(c1).

In addition, in Fig. 3(c2) for coherences, the extracted results significantly deviate from the true $\rho_{ij}(\tau)$ ($i \neq j$). All these deviations suggest additional postprocess be required to obtain the correct $\rho_{ij}(\tau)$. Therefore, we introduce the reconstruction protocol utilizing both the THz-free and THz-streaking $w(p; \tau)$ to effectively eliminate the contributions from surrounding peaks (see Supplemental Material [14], Sec. III). Then, after applying quantum jump correction (which only slightly influences results in our situation; details will be discussed in the subsequent work), the reconstructed $\rho_{ij}(\tau)$ are shown in Fig. 3(d) comparing with the true $\rho_{ij}(\tau)$. Except for the poor agreement around t_0 as resolving the fast excitation dynamics is restricted by the relatively large XUV pulse duration, the reconstructed $\rho_{ij}(\tau)$ from the simulated measurement well recovers the true $\rho_{ij}(\tau)$, validating the feasibility of density matrix reconstruction using streaking-assisted photoelectron spectra.

In summary, a spectroscopic protocol is proposed to describe time-evolved density matrix elements, which can be reconstructed from the streaking-assisted photoelectron spectrum. With the XUV pulse of fs scale width, the beating of the quantum coherence can be retrieved with the sub-fs precision, less restricted by the duration of probing field than in conventional transient spectroscopies. The analysis of the process is substantially simplified by a model with the spectral distribution described by the sum over Gaussian peaks, whose characteristic momenta effectively separate all density matrix elements. The model also indicates that the spectrum oscillates with p near p_{ij}, providing an innovative approach to relative-phase reconstruction at arbitrary time. Above all, the systematic protocol of $\rho_{ij}(\tau)$-reconstruction is demonstrated by simulated measurement observing the excitation and decoherence dynamics in a multilevel open system, showing the potential applicability to study general ultrafast coherence dynamics in complex systems.

[*] yantm@sari.ac.cn

[†] jiangyh@sari.ac.cn

[1] S. Pabst, L. Greenman, P. J. Ho, D. A. Mazziotti, and R. Santra, Phys. Rev. Lett. **106**, 053003 (2011).

[2] C. Arnold, O. Vendrell, and R. Santra, Phys. Rev. A **95**, 033425 (2017).

[3] G. S. Engel, T. R. Calhoun, E. L. Read, T.-K. Ahn, T. Mančal, Y.-C. Cheng, R. E. Blankenship, and G. R. Fleming, Nature (London) **446**, 782 (2007).

[4] E. Collini and G. D. Scholes, Science **323**, 369 (2009).

[5] E. Collini, C. Y. Wong, K. E. Wilk, P. M. G. Curmi, P. Brumer, and G. D. Scholes, Nature (London) **463**, 644 (2010).

[6] J. Yuen-Zhou, J. J. Krich, M. Mohseni, and A. Aspuru-Guzik, Proc. Natl. Acad. Sci. U.S.A. **108**, 17615 (2011).

[7] E. Goulielmakis, Z.-H. Loh, A. Wirth, R. Santra, N. Rohringer, V. S. Yakovlev, S. Zherebtsov, T. Pfeifer, A. M. Azzeer, M. F. Kling, S. R. Leone, and F. Krausz, Nature (London) **466**, 739 (2010).

[8] C. Ott, A. Kaldun, L. Argenti, P. Raith, K. Meyer, M. Laux, Y. Zhang, A. Blättermann, S. Hagstotz, T. Ding, R. Heck, J. Madroñero, F. Martín, and T. Pfeifer, Nature (London) **516**, 374 (2014).

[9] M. Kowalewski, K. Bennett, J. R. Rouxel, and S. Mukamel, Phys. Rev. Lett. **117**, 043201 (2016).

[10] W. Helml, A. R. Maier, W. Schweinberger, I. Grguraš, P. Radcliffe, G. Doumy, C. Roedig, J. Gagnon, M. Messerschmidt, S. Schorb, C. Bostedt, F. Grüner, L. F. DiMauro, D. Cubaynes, J. D. Bozek, T. Tschentscher, J. T. Costello, M. Meyer, R. Coffee, S. Düsterer et al., Nat. Photonics **8**, 950 (2014).

[11] R. Kienberger, M. Hentschel, M. Uiberacker, C. Spielmann, M. Kitzler, A. Scrinzi, M. Wieland, T. Westerwalbesloh, U. Kleineberg, U. Heinzmann, M. Drescher, and F. Krausz, Science **297**, 1144 (2002).

[12] U. Frühling, M. Wieland, M. Gensch, T. Gebert, B. Schütte, M. Krikunova, R. Kalms, F. Budzyn, O. Grimm, J. Rossbach, E. Plönjes, and M. Drescher, Nat. Photonics **3**, 523 (2009).

[13] I. Grguraš, A. R. Maier, C. Behrens, T. Mazza, T. J. Kelly, P. Radcliffe, S. Düsterer, A. K. Kazansky, N. M. Kabachnik, T. Tschentscher, J. T. Costello, M. Meyer, M. C. Hoffmann, H. Schlarb, and A. L. Cavalieri, Nat. Photonics **6**, 852 (2012).

[14] See Supplemental Material at http://link.aps.org/supplemental/10.1103/PhysRevLett.121.113201 for the details about the derivation of formulas, numerical simulation, and the $\rho_{ij}(\tau)$-reconstruction procedure.

[15] S. Ackermann, A. Azima, S. Bajt, J. Bödewadt, F. Curbis, H. Dachraoui, H. Delsim-Hashemi, M. Drescher, S. Düsterer, B. Faatz, M. Felber, J. Feldhaus, E. Hass, U. Hipp, K. Honkavaara, R. Ischebeck, S. Khan, T. Laarmann, C. Lechner, T. Maltezopoulos et al., Phys. Rev. Lett. **111**, 114801 (2013).

[16] J. Dalibard, Y. Castin, and K. Mølmer, Phys. Rev. Lett. **68**, 580 (1992).